# Molecular Docking Analysis of Flavonoid Compounds from *Glycyrrhiza glabra* on the Interleukin – 1 Receptor (IL-1R) as a Candidate for Anti-Inflammatory Drug in Periodontitis

Elza Ibrahim Auerkari *, Samantha Ruth Andriawan , Pertti Auerkari

Posted Date: 24 November 2023

doi: 10.20944/preprints202311.1542.v1

Keywords: IL-1R; Interleukin–1 receptor; Il-1 receptor; Glycyrrhiza glabra; Licorice; Flavonoid; Inflammation; Periodontitis; Molecular docking; In silico

*Article*

# Molecular Docking Analysis of Flavonoid Compounds from *Glycyrrhiza Glabra* on the Interleukin—1 Receptor (IL-1R) as A Candidate for Anti-Inflammatory Drug in Periodontitis

**Elza Ibrahim Auerkari [1,*], Samantha Ruth Andriawan [1] and Pertti Auerkari [2]**

[1] Department of Oral Biology, Faculty of Dentistry, University of Indonesia, Jakarta, Indonesia
[2] Department of Mechanical Engineering, School of Engineering, Aalto University, Espoo, Finland
* Correspondence: Eauerkari@Yahoo.Com

**Abstract:** Periodontitis is a disease that originates from gingival tissue, and if left untreated, can cause inflammation to spread to deeper tissues, altering bone homeostasis, and even leading to tooth loss. When the bacteria in plaque reach sufficient numbers, the immune system responds by activating immune cells that will produce cytokines, including interleukin-1 (IL-1), interleukin-6 (IL-6), and tumor necrosis factor-alpha (TNF-$\alpha$). These immune signaling molecules will coordinate the inflammatory responses. IL-1 binds to the IL-1 receptor (IL-1R) on the surface of target cells, initiating an inflammatory response by activating intracellular signalling pathways. Inhibition of IL-1R can prevent the interaction of IL-1 with this receptor, thereby halting the activation of the inflammatory pathway. By substituting this connection with active anti-inflammatory substances, it is possible to prevent the contact between IL-1 and IL-1R. The licorice plant, *Glycyrrhiza glabra*, includes eight types of flavonoids with significant anti-inflammatory potential, namely isoliquiritigenin, glyzaglabrin, prunetin, shinpterocarpin, licochalcone A, glabridin, glisoflavone, and isoangustone A. This study aims to assess the potential of such flavonoids as candidates for periodontitis treatment through molecular docking, using *AutoDock Tools v.1.5.6*. All tested compounds showed highly stable bonds to IL-1R, with a binding affinity values below -7 kcal/mol. *Van der Waals* forces, hydrogen bonds, and hydrophobic bonds all contribute to the stability of these interactions. Among the eight tested compounds, glisoflavone, which has a Ki value of 90.89 nM and a $\Delta$G value of -9.61 kcal/mol, has the highest binding stability to IL-1R.

**Keywords:** IL-1R; Interleukin–1 receptor; Il-1 receptor; *Glycyrrhiza glabra*; Licorice; Flavonoid; Inflammation; Periodontitis; Molecular docking; *In silico*

## INTRODUCTION

Periodontitis is a disease that originates from gingival tissue, and if left untreated, can cause inflammation to spread to deeper tissues, altering bone homeostasis, and even leading to tooth loss [1]. Around 19% of adults globally are thought to have severe periodontal diseases, which amounts to more than 1 billion cases worldwide, while about 74% of Indonesian adults have periodontitis [2,3]. The etiology of periodontal disease is multifactorial. The bacterial biofilm developing on the tooth surfaces has been recognized as the primary cause of periodontitis. *Porphyromonas gingivalis*, *Treponema denticola*, *Aggregatibacter actinomycetemcomitans*, and *Tannerella forsythia* are the pathogens linked to periodontitis [4]. Mixed bacterial colonization in the oral tissue is the main factor causing periodontal disease [5,6]. While other factors, such as developmental grooves, calculus, dental plaque, overhanging restorations, anatomical features like the short trunk, cervical enamel projections, systemic factors, genetic factors, smoking, and stress, act as secondary etiologic factors accelerating the spread and development of periodontal diseases [7]. When the bacteria in plaque reach sufficient numbers, the immune system responds by activating immune cells such as macrophages, neutrophils, and dendritic cells to combat the bacterial infection. The activated immune cells in this response produce cytokines, including interleukin-1 (IL-1), interleukin-6 (IL-6), and tumor necrosis factor-alpha (TNF-$\alpha$). These cytokines play a role in regulating the inflammatory

 doi:10.20944/preprints202311.1542.v1



response and stimulating inflammation reactions. The inflammatory response is the body's effort to destroy bacteria within the plaque. Immune cells flow to the infected area, and blood vessels in that area widen, causing swelling, redness, and increased blood flow [8].

Interleukin-1 is a type of cytokine, which are immune signalling molecules used to coordinate inflammatory responses. There are two main forms of IL-1, namely IL-1$\alpha$ and IL-1$\beta$. They play a crucial role in regulating inflammation and triggering the immune response to infections. IL-1 binds to the IL-1 receptor (IL-1R) on the surface of target cells, initiating an inflammatory response by activating intracellular signalling pathways. Inhibition of IL-1R can prevent the interaction of IL-1 with this receptor, thereby halting the activation of the inflammatory pathway [9]. By substituting this connection with active substances that have anti-inflammatory potential, it is possible to prevent the contact between IL-1 and IL-1R. The licorice plant, *Glycyrrhiza glabra*, is thought to contain such substances. The plant grows in Indonesia and apart from local availability and possible therapeutic potential has the further advantage of minimal disturbance to human physiological activities [10].

Several studies have identified the licorice plant as a source of antioxidants, antidepressants, anti-inflammatory compounds, and antimicrobial, antitussive, antiviral , antiulcer , and anticancer agents [11–16]. Within this plant, various active compounds are present, such as flavonoids, coumarins, saponins, propionic acid, benzoic acid, ethyl linoleate, and triterpenoids. However, the primary benefits of the plant are mainly derived from its flavonoid compounds [17,18]. In licorice, there are eight types of flavonoids with significant anti-inflammatory potential, namely isoliquiritigenin, glyzaglabrin, prunetin, shinpterocarpin, licochalcone A, glabridin, glisoflavone, and isoangustone A [19–26]. Given that they share molecular structures with glucocorticoids, these flavonoids stimulate the signalling of glucocorticoid receptors and inhibit the classical complement pathway, both of which features are responsible for their anti-inflammatory effects. Additionally, preclinical research has demonstrated that these flavonoids decrease prostaglandin synthesis, cyclooxygenase activity, and indirectly inhibit platelet aggregation and the elements of the inflammatory cascade. Not only that, these flavonoids can inhibit the interaction of IL-1R with IL-1, thus stopping the activation of the inflammatory pathway [4].

In drug development research, the typical stages that need to be traversed include in vitro testing, in vivo testing on test animals, in vivo testing, followed by clinical trials before eventually allowing use in general [27]. These stages come with various limitations such as high costs, lengthy durations, and uncertain success rates [28]. These limitations can be addressed through *in silico* research methods. *In silico* research is conducted using computational or computer-based techniques, and it is especially useful when laboratory experiments are expensive, hazardous, or difficult to conduct, and for comprehending phenomena that are too complex to be directly tested [29] *In silico* research assists researchers in making more accurate predictions to enhance the success rate of a study before *in vitro* and *in vivo* research is conducted [29,30].

*In silico* research is closely linked with the field of molecular biology that studies the structure, function, and interactions of biological molecules within cells [30]. One type of *in silico* research is molecular docking. The primary goal of molecular docking is to understand how two molecules interact and predict the binding strength between the receptor and the ligand [31,32]. In the present context, molecular docking can be employed to predict the binding strength between Il-1 receptor (IL-1R) and flavonoid compounds to compete with binding to Il-1 [32].

In this paper, the analysis aims to assess the potential of flavonoids of *Glycyrrhiza glabra*, as a source of medicinal materials, particularly as candidates for anti-inflammatory drugs in periodontitis.

## MATERIALS AND METHODS

### *Hardware*

The hardware used was a personal computer, Lenovo IdeaPad Slim 3i, equipped with an Intel® Core™ i3 processor and running on the Windows 11 operating system.

 doi:10.20944/preprints202311.1542.v1



*Software*

AutoDock Tools version 1.5.6, BIOVIA Discovery Studio Visualizer v.21, and ChemDraw Professional 16.0 were the programs used in this study.

*Protein Structure Preparation*

In this study, the protein structure used is the IL-1 receptor (IL-1R) with PDBID 6MOM. This structure was chosen because of its high resolution. Using the *BIOVIA Discovery Studio Visualizer v.21 program*, this protein underwent a simulated purification process to remove water molecules and the native ligands, leaving only the pure protein structure. Subsequently, the protein resulting from the purification process underwent a series of preparation steps using the *AutoDockTools v.1.5.6* program, including the addition of Kollman charges and polar hydrogen atoms. Thus, the purification and preparation processes of the IL-1R structure have been completed.

*Ligand Structures Preparation*

In this study, eight flavonoid compounds were used as test ligands, namely isoliquiritigenin, glyzaglabrin, prunetin, shinpterocarpin, licochalcone A, glabridin, glisoflavone, and isoangustone A. These eight compounds needed to undergo a series of preparation processes before being used for docking simulations. The first step to be taken was the energy minimization of these test compounds using the *ChemDraw Professional 16.0* program. Subsequently, the compounds that have undergone energy minimization were prepared using the *AutoDockTools v.1.5.6* program, with Gasteiger charges calculation, the addition of both polar and non-polar hydrogen atoms, as well as the merging of non-polar molecules. Thus, the preparation process of the ligand structures of the test compounds was complete, and the docking process was ready to begin.

*Molecular Docking Simulation*

To dock the ligands into the targets, the primary program used was *AutoDockTools v.1.5.6*. The first step was to input the protein structure and the ligands that had been prepared simultaneously. Next, grid point parametrization was performed, with a grid box size of 40 x 40 x 40 Å and grid coordinates of x = 23.986; y = 10.551; z = 32.024. The parameters used in the docking of this study involved a genetic algorithm with a total of 100 docking attempts for each compound. Upon completion of the docking process, several important pieces of information were obtained, including binding affinity, inhibition concentration, and a clustering histogram table. The *BIOVIA Discovery Studio Visualizer v.21* program was used as well to visualize the 2-dimensional interactions between the tested ligands and the IL-1 receptor (IL-1R). This program allowed us to obtain information regarding which amino acids of the target protein bind with the ligand, complete with the types of bonds formed.

## RESULTS AND DISCUSSION

The docking results between the ligands and IL-1R are shown in Figures 1–8.

Preprints (www.preprints.org) | NOT PEER-REVIEWED | Posted: 24 November 2023 doi:10.20944/preprints202311.1542.v1



CLUSTERING HISTOGRAM

| Cluster Rank | Lowest Binding Energy | Run | Mean Binding Energy | Num in Clus | Histogram (5 10 15 20 25 30 35) |
|---|---|---|---|---|---|
| 1 | -8.32 | 53 | -7.93 | 77 | ################################################################################ |
| 2 | -8.08 | 100 | -7.52 | 20 | #################### |
| 3 | -7.17 | 30 | -7.17 | 1 | # |
| 4 | -6.87 | 82 | -6.87 | 1 | # |
| 5 | -6.72 | 1 | -6.72 | 1 | # |

(**A**)

FINAL GENETIC ALGORITHM DOCKED STATE

```
Detailed state:  trans 23.133 9.735 33.666 quatxyzw -0.479253 -0.049326 -0.852420 -0.203135 center 1.594 0.211 -0.134 ntor 6 22.2258 -152.1478 114.6454
20.7772 104.0078 -39.9467
State:   23.133   9.735  33.666  -0.489 -0.050 -0.871 -156.559     22.23 -152.15  114.65   20.78  104.01  -39.95

DOCKED: MODEL       53
DOCKED: USER    Run = 53
DOCKED: USER    DPF = dock.dpf
DOCKED: USER
DOCKED: USER    Estimated Free Energy of Binding    =   -8.32 kcal/mol  [=(1)+(2)+(3)-(4)]
DOCKED: USER    Estimated Inhibition Constant, Ki   =  799.16 nM (nanomolar)  [Temperature = 298.15 K]
DOCKED: USER
DOCKED: USER    (1) Final Intermolecular Energy     =  -10.11 kcal/mol
DOCKED: USER        vdW + Hbond + desolv Energy     =   -9.61 kcal/mol
DOCKED: USER        Electrostatic Energy            =   -0.49 kcal/mol
DOCKED: USER    (2) Final Total Internal Energy     =   -0.99 kcal/mol
DOCKED: USER    (3) Torsional Free Energy           =   +1.79 kcal/mol
DOCKED: USER    (4) Unbound System's Energy  [=(2)] =   -0.99 kcal/mol
DOCKED: USER
```

(**B**)

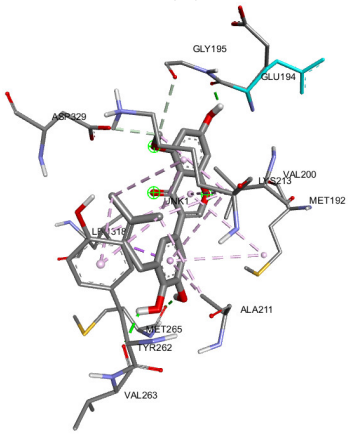


(**C**)

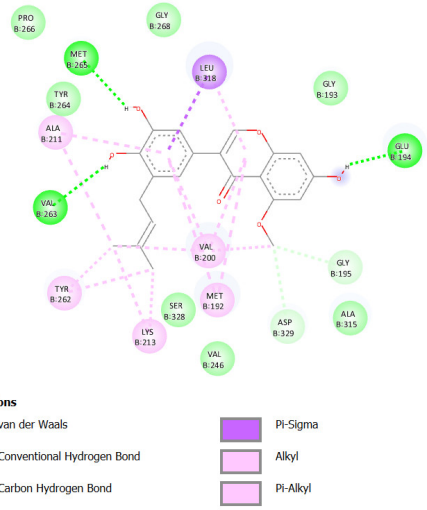


(**D**)

Preprints (www.preprints.org) | NOT PEER-REVIEWED | Posted: 24 November 2023 doi:10.20944/preprints202311.1542.v1



**Figure 1.** Docking results of isoliquiritigenin with IL-1R (**A**) Histogram of docking results between isoliquiritigenin and IL-1R; (**B**) Best pose in the molecular docking between isoliquiritigenin and IL-1R; (**C**) 3D shape of the interaction between isoliquiritigenin and IL-1R as viewed through the *BIOVIA Discovery Studio Visualizer v.21*; (**D**) 2D representation of the interaction between isoliquiritigenin and IL-1R as viewed through the *BIOVIA Discovery Studio Visualizer v.21*.

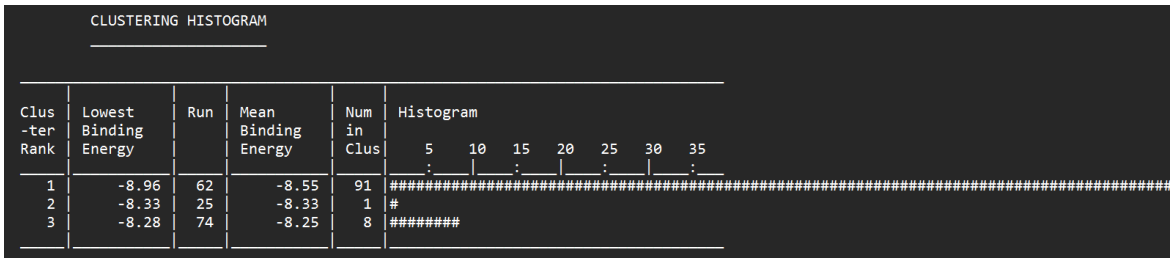


(**A**)

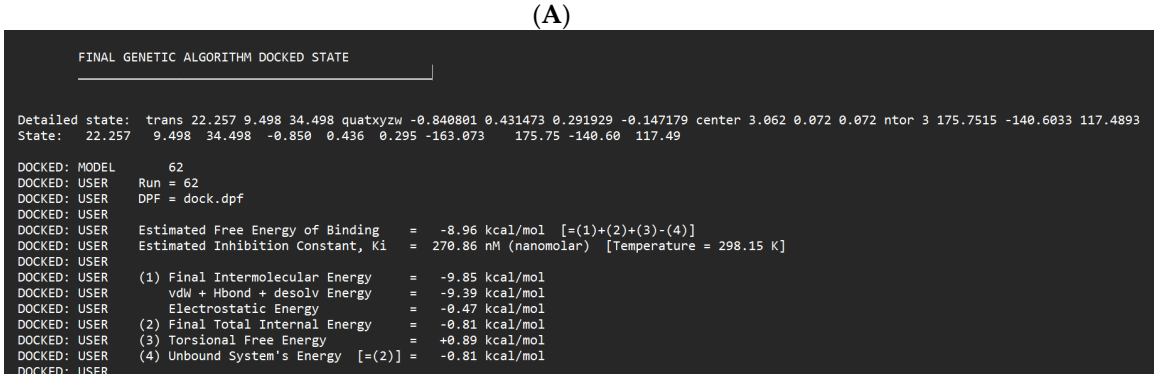


(**B**)

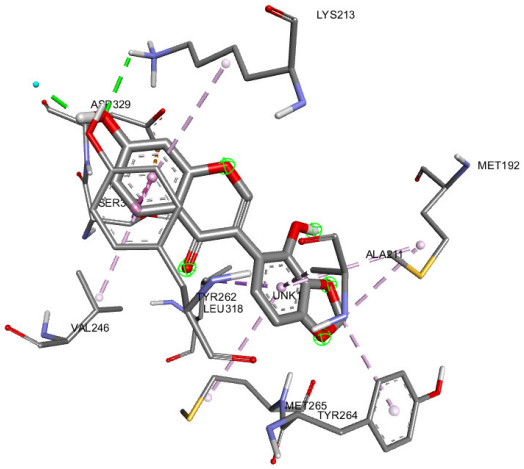


(**C**)

Preprints (www.preprints.org) | NOT PEER-REVIEWED | Posted: 24 November 2023 doi:10.20944/preprints202311.1542.v1



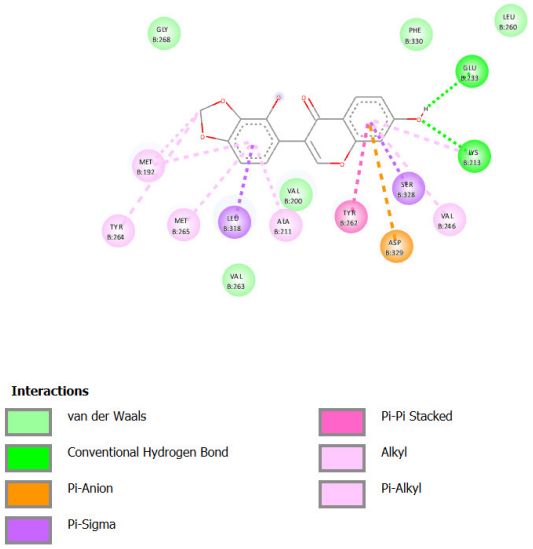


(**D**)

**Figure 2.** Docking Results of Glyzaglabrin with IL-1R; (**A**) Histogram of Docking Results; (**B**) Best Pose In The Molecular Docking; (**C**) 3D Shape of The Interaction As Viewed Through The *BIOVIA Discovery Studio Visualizer V.21*; (**D**) 2D Representation of The Interaction.

```
        CLUSTERING HISTOGRAM
        ____________________

_____________________________________________________________________________
|     |           |     |           |     |
Clus  | Lowest    | Run | Mean      | Num | Histogram
-ter  | Binding   |     | Binding   | in  |
Rank  | Energy    |     | Energy    | Clus|    5    10   15   20   25   30   35
_____|___________|_____|___________|_____|____:____|____:____|____:____|____:____|___
   1 |     -8.40 |   4 |     -8.22 |  99 |##################################################################################################
   2 |     -7.75 |  47 |     -7.75 |   1 |#
_____|___________|_____|___________|_____|_____________________________________________
```

(**A**)

```
        FINAL GENETIC ALGORITHM DOCKED STATE
        ____________________________________


Detailed state:  trans 22.911 9.158 33.877 quatxyzw 0.396763 0.083141 0.886995 -0.221149 center 3.804 0.307 0.012 ntor 4 -112.5451 -144.8177 -45.5512
123.1844
State:   22.911   9.158  33.877   0.407  0.085  0.910 -154.447   -112.55 -144.82  -45.55  123.18

DOCKED: MODEL        4
DOCKED: USER    Run = 4
DOCKED: USER    DPF = dock.dpf
DOCKED: USER
DOCKED: USER    Estimated Free Energy of Binding    =   -8.40 kcal/mol  [=(1)+(2)+(3)-(4)]
DOCKED: USER    Estimated Inhibition Constant, Ki   =  691.20 nM (nanomolar)  [Temperature = 298.15 K]
DOCKED: USER
DOCKED: USER    (1) Final Intermolecular Energy     =   -9.60 kcal/mol
DOCKED: USER        vdW + Hbond + desolv Energy     =   -9.49 kcal/mol
DOCKED: USER        Electrostatic Energy            =   -0.11 kcal/mol
DOCKED: USER    (2) Final Total Internal Energy     =   -1.01 kcal/mol
DOCKED: USER    (3) Torsional Free Energy           =   +1.19 kcal/mol
DOCKED: USER    (4) Unbound System's Energy  [=(2)] =   -1.01 kcal/mol
```

(**B**)

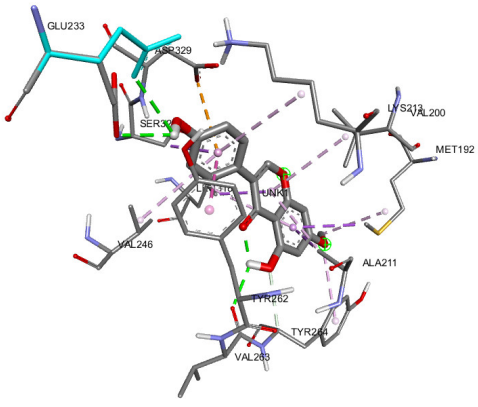


(**C**)

Preprints (www.preprints.org) | NOT PEER-REVIEWED | Posted: 24 November 2023 doi:10.20944/preprints202311.1542.v1



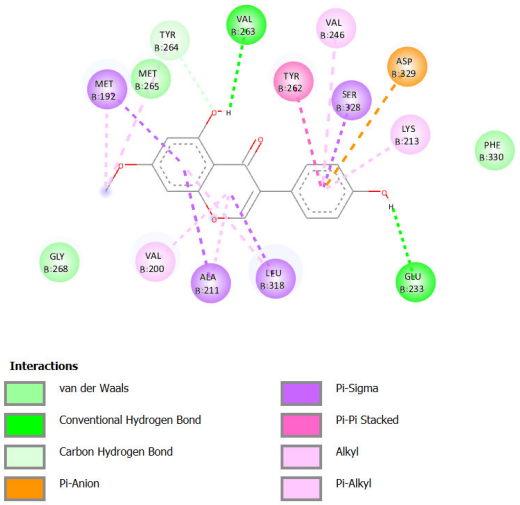


(**D**)

**Figure 3.** Docking Results of Prunetin with IL-1R; (**A**) Histogram of Docking Results; (**B**) Best Pose In The Molecular Docking; (**C**) 3D Shape of The Interaction As Viewed Through The *BIOVIA Discovery Studio Visualizer V.21*; (**D**) 2D Representation of The Interaction.

```
        CLUSTERING HISTOGRAM
        ____________________

_____|____________|_____|____________|_____|_____________________________________________________
Clus | Lowest     | Run | Mean       | Num | Histogram
-ter | Binding    |     | Binding    | in  |
Rank | Energy     |     | Energy     | Clus|    5    10   15   20   25   30   35
_____|____________|_____|____________|_____|____:____|____:____|____:____|____:___
   1 |      -9.32 |   7 |      -9.31 |  67 |#################################################################
   2 |      -9.22 |  46 |      -9.22 |  33 |#################################
_____|____________|_____|____________|_____|_____________________________________________________
```

(**A**)

```
        FINAL GENETIC ALGORITHM DOCKED STATE
        ____________________________________


Detailed state:  trans 23.008 10.773 33.379 quatxyzw 0.137406 -0.842334 -0.210687 -0.476659 center 3.057 0.252 0.162 ntor 1 148.6
State:   23.008  10.773  33.379   0.156 -0.958 -0.240 -123.065    148.02

DOCKED: MODEL        7
DOCKED: USER    Run = 7
DOCKED: USER    DPF = dock.dpf
DOCKED: USER
DOCKED: USER    Estimated Free Energy of Binding    =   -9.32 kcal/mol  [=(1)+(2)+(3)-(4)]
DOCKED: USER    Estimated Inhibition Constant, Ki   =  148.30 nM (nanomolar)  [Temperature = 298.15 K]
DOCKED: USER
DOCKED: USER    (1) Final Intermolecular Energy     =   -9.61 kcal/mol
DOCKED: USER        vdW + Hbond + desolv Energy     =   -9.30 kcal/mol
DOCKED: USER        Electrostatic Energy            =   -0.31 kcal/mol
DOCKED: USER    (2) Final Total Internal Energy     =   +0.02 kcal/mol
DOCKED: USER    (3) Torsional Free Energy           =   +0.30 kcal/mol
DOCKED: USER    (4) Unbound System's Energy  [=(2)] =   +0.02 kcal/mol
DOCKED: USER
```

(**B**)

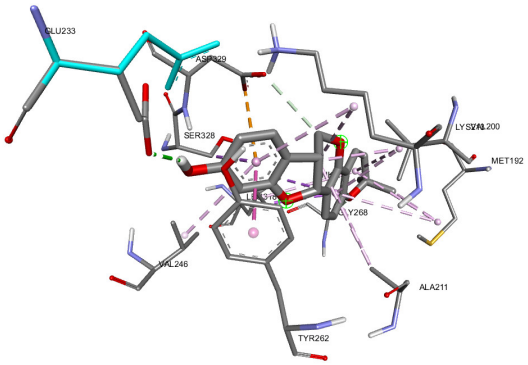


(**C**)

Preprints (www.preprints.org) | NOT PEER-REVIEWED | Posted: 24 November 2023 doi:10.20944/preprints202311.1542.v1



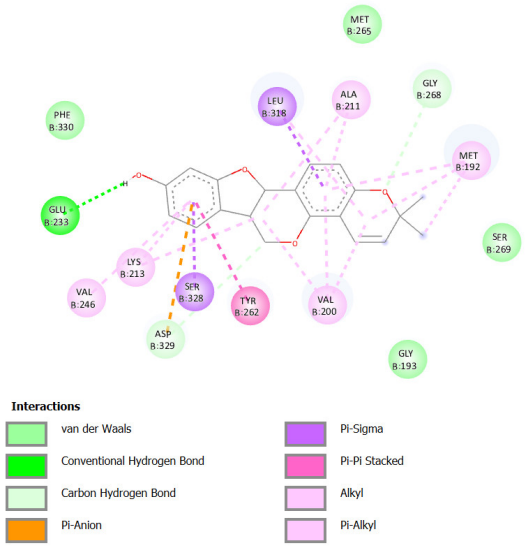


(**D**)

**Figure 4.** Docking Results of Shinpterocarpin with IL-1R; (A) Histogram of Docking Results; (B) Best Pose In The Molecular Docking; (C) 3D Shape of The Interaction As Viewed Through The *BIOVIA Discovery Studio Visualizer V.21*; (D) 2D Representation of The Interaction.

CLUSTERING HISTOGRAM

| Clus-ter Rank | Lowest Binding Energy | Run | Mean Binding Energy | Num in Clus | Histogram 5 10 15 20 25 30 35 |
|---|---|---|---|---|---|
| 1 | -9.68 | 82 | -9.46 | 4 | #### |
| 2 | -9.08 | 38 | -8.41 | 24 | ######################## |
| 3 | -9.06 | 83 | -8.51 | 6 | ###### |
| 4 | -8.65 | 65 | -8.39 | 16 | ################ |
| 5 | -8.54 | 21 | -8.30 | 3 | ### |
| 6 | -8.47 | 84 | -8.26 | 4 | #### |
| 7 | -8.44 | 88 | -8.30 | 5 | ##### |
| 8 | -8.35 | 95 | -8.28 | 2 | ## |
| 9 | -8.33 | 19 | -8.21 | 13 | ############# |
| 10 | -8.33 | 68 | -8.33 | 1 | # |
| 11 | -8.07 | 10 | -7.86 | 18 | ################## |
| 12 | -7.61 | 98 | -7.59 | 4 | #### |

(**A**)

FINAL GENETIC ALGORITHM DOCKED STATE

```
Detailed state:  trans 23.363 11.388 33.272 quatxyzw 0.825137 -0.247697 -0.505854 0.043657 center 2.853 -0.330 0.018 ntor 8 -45.1439 -159.4783 123.9687
18.3465 31.8200 -151.2024 52.7839 31.1740
State:   23.363  11.388  33.272   0.826 -0.248 -0.506 174.996    -45.14 -159.48  123.97   18.35   31.82 -151.20   52.78   31.17

DOCKED: MODEL       38
DOCKED: USER    Run = 38
DOCKED: USER    DPF = dock.dpf
DOCKED: USER
DOCKED: USER    Estimated Free Energy of Binding    =   -9.08 kcal/mol  [=(1)+(2)+(3)-(4)]
DOCKED: USER    Estimated Inhibition Constant, Ki   =  219.85 nM (nanomolar)  [Temperature = 298.15 K]
DOCKED: USER
DOCKED: USER    (1) Final Intermolecular Energy     =  -11.47 kcal/mol
DOCKED: USER        vdW + Hbond + desolv Energy     =  -11.09 kcal/mol
DOCKED: USER        Electrostatic Energy            =   -0.38 kcal/mol
DOCKED: USER    (2) Final Total Internal Energy     =   -1.20 kcal/mol
DOCKED: USER    (3) Torsional Free Energy           =   +2.39 kcal/mol
DOCKED: USER    (4) Unbound System's Energy  [=(2)] =   -1.20 kcal/mol
```

(**B**)

Preprints (www.preprints.org) | NOT PEER-REVIEWED | Posted: 24 November 2023 doi:10.20944/preprints202311.1542.v1



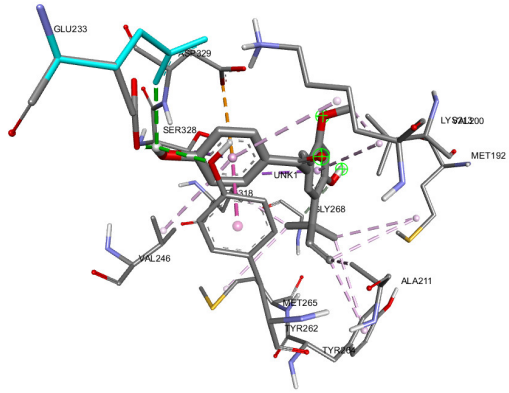


(**C**)

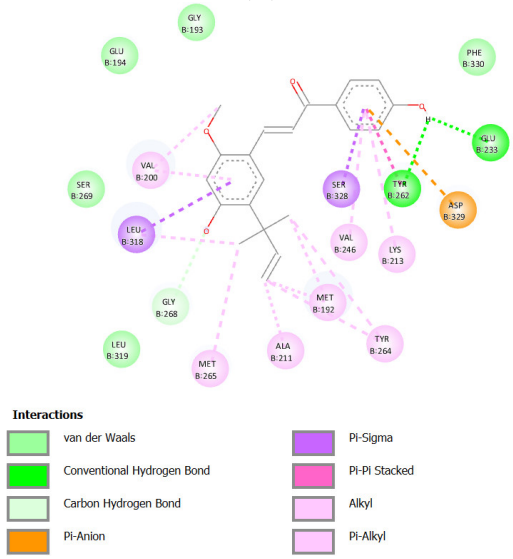


(**D**)

**Figure 5.** Docking Results of Licochalcone A with IL-1R; (**A**) Histogram of Docking Results; (**B**) Best Pose In The Molecular Docking; (**C**) 3D Shape of The Interaction As Viewed Through The *BIOVIA Discovery Studio Visualizer V.21*; (**D**) 2D Representation of The Interaction.

```
        CLUSTERING HISTOGRAM
        ____________________

_____________________________________________________________________________
|      |            |     |            |     |                               |
Clus   | Lowest     | Run | Mean       | Num | Histogram                     |
-ter   | Binding    |     | Binding    | in  |                               |
Rank   | Energy     |     | Energy     | Clus|    5    10   15   20   25   30   35
_______|____________|_____|____________|_____|____:____|____:____|____:____|____:___
   1   |      -8.93 |  97 |      -8.67 |  68 |#################################################################
   2   |      -8.45 |  37 |      -8.31 |   2 |##
   3   |      -8.42 |  59 |      -8.36 |  19 |###################
   4   |      -8.30 |  68 |      -8.29 |  11 |###########
_______|____________|_____|____________|_____|_____________________________________
```

(**A**)

```
        FINAL GENETIC ALGORITHM DOCKED STATE
        ____________________________________


Detailed state:  trans 24.234 9.646 32.454 quatxyzw 0.403038 -0.414098 0.062849 0.813716 center 4.016 -0.151 0.202 ntor 3 17.7831 153.5458 141.1580
State:   24.234   9.646  32.454   0.693 -0.712  0.108 71.079     17.78  153.55  141.16

DOCKED: MODEL       97
DOCKED: USER    Run = 97
DOCKED: USER    DPF = dock.dpf
DOCKED: USER
DOCKED: USER    Estimated Free Energy of Binding    =   -8.93 kcal/mol  [=(1)+(2)+(3)-(4)]
DOCKED: USER    Estimated Inhibition Constant, Ki   =  283.04 nM (nanomolar)  [Temperature = 298.15 K]
DOCKED: USER
DOCKED: USER    (1) Final Intermolecular Energy     =   -9.83 kcal/mol
DOCKED: USER        vdW + Hbond + desolv Energy     =   -9.67 kcal/mol
DOCKED: USER        Electrostatic Energy            =   -0.16 kcal/mol
DOCKED: USER    (2) Final Total Internal Energy     =   +0.22 kcal/mol
DOCKED: USER    (3) Torsional Free Energy           =   +0.89 kcal/mol
DOCKED: USER    (4) Unbound System's Energy  [=(2)] =   +0.22 kcal/mol
DOCKED: USER
```

(**B**)

Preprints (www.preprints.org) | NOT PEER-REVIEWED | Posted: 24 November 2023 doi:10.20944/preprints202311.1542.v1



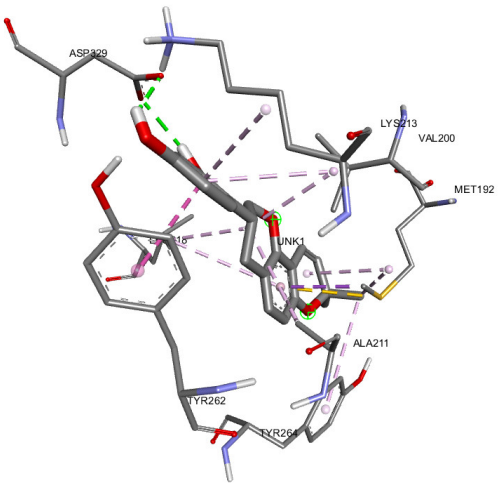


(**C**)

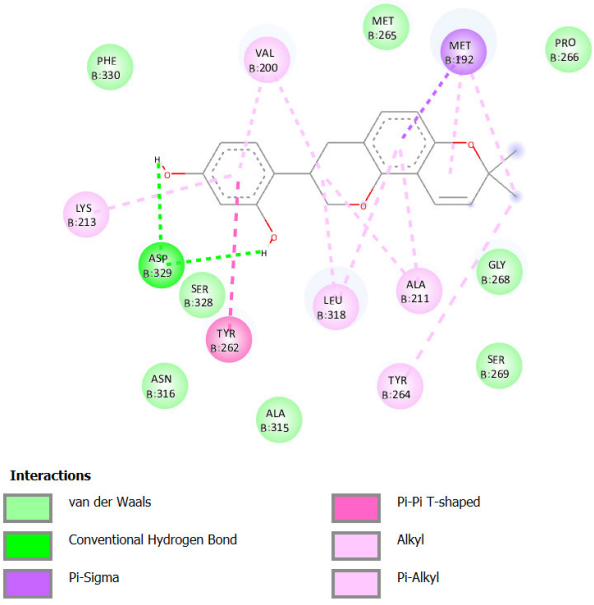


(**D**)

**Figure 6.** Docking Results of Glabridin with IL-1R; (**A**) Histogram of Docking Results; (**B**) Best Pose In The Molecular Docking; (**C**) 3D Shape of The Interaction As Viewed Through The *BIOVIA Discovery Studio Visualizer V.21*; (**D**) 2D Representation of The Interaction.

CLUSTERING HISTOGRAM

| Clus-ter Rank | Lowest Binding Energy | Run | Mean Binding Energy | Num in Clus | Histogram 5 10 15 20 25 30 35 |
|---|---|---|---|---|---|
| 1 | -9.72 | 72 | -9.32 | 31 | ################################ |
| 2 | -9.61 | 12 | -8.95 | 36 | ##################################### |
| 3 | -9.00 | 54 | -8.84 | 3 | ### |
| 4 | -8.90 | 36 | -8.58 | 11 | ########### |
| 5 | -8.89 | 96 | -8.81 | 4 | #### |
| 6 | -8.76 | 33 | -8.76 | 1 | # |
| 7 | -8.70 | 89 | -8.46 | 12 | ############ |
| 8 | -8.64 | 73 | -8.40 | 2 | ## |

(**A**)

Preprints (www.preprints.org) | NOT PEER-REVIEWED | Posted: 24 November 2023 doi:10.20944/preprints202311.1542.v1



```
        FINAL GENETIC ALGORITHM DOCKED STATE
        ____________________________________


Detailed state:  trans 23.903 10.431 32.099 quatxyzw -0.503804 0.823661 0.142043 0.218147 center 3.965 -0.595 0.205 ntor
7 -107.4769 -64.0025 -58.8137 -114.0916 154.5160 -75.8580 2.1346
State:   23.903  10.431  32.099  -0.516  0.844  0.146 154.800   -107.48  -64.00  -58.81 -114.09  154.52  -75.86    2.13

DOCKED: MODEL       12
DOCKED: USER    Run = 12
DOCKED: USER    DPF = dock.dpf
DOCKED: USER
DOCKED: USER    Estimated Free Energy of Binding    =   -9.61 kcal/mol  [=(1)+(2)+(3)-(4)]
DOCKED: USER    Estimated Inhibition Constant, Ki   =   90.89 nM (nanomolar)  [Temperature = 298.15 K]
DOCKED: USER
DOCKED: USER    (1) Final Intermolecular Energy     =  -11.69 kcal/mol
DOCKED: USER        vdW + Hbond + desolv Energy     =  -11.54 kcal/mol
DOCKED: USER        Electrostatic Energy            =   -0.15 kcal/mol
DOCKED: USER    (2) Final Total Internal Energy     =   -1.26 kcal/mol
DOCKED: USER    (3) Torsional Free Energy           =   +2.09 kcal/mol
DOCKED: USER    (4) Unbound System's Energy  [=(2)] =   -1.26 kcal/mol
DOCKED: USER
```

(**B**)

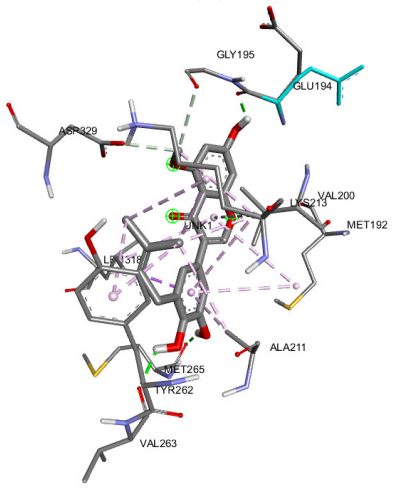


(**C**)

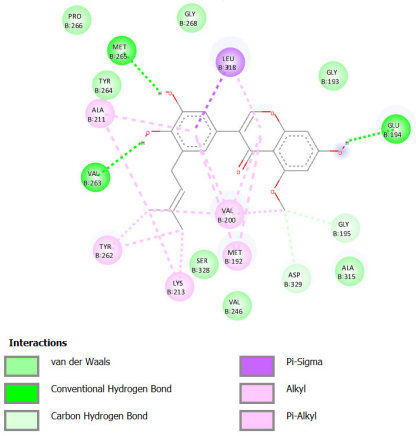


(**D**)

**Figure 7.** Docking Results of Glisoflavone with IL-1R; (**A**) Histogram of Docking Results; (**B**) Best Pose In The Molecular Docking; (**C**) 3D Shape of The Interaction As Viewed Through The *BIOVIA Discovery Studio Visualizer V.21*; (**D**) 2D Representation of The Interaction.

Preprints (www.preprints.org) | NOT PEER-REVIEWED | Posted: 24 November 2023 doi:10.20944/preprints202311.1542.v1



CLUSTERING HISTOGRAM

| Clus-ter Rank | Lowest Binding Energy | Run | Mean Binding Energy | Num in Clus | Histogram 5 10 15 20 25 30 35 |
|---|---|---|---|---|---|
| 1 | -9.68 | 66 | -8.85 | 8 | ######## |
| 2 | -9.52 | 75 | -9.25 | 21 | ###################### |
| 3 | -9.35 | 41 | -8.82 | 27 | ########################### |
| 4 | -9.17 | 34 | -8.76 | 18 | ################## |
| 5 | -9.15 | 73 | -8.40 | 8 | ######## |
| 6 | -9.00 | 87 | -8.42 | 7 | ####### |
| 7 | -8.39 | 68 | -8.39 | 1 | # |
| 8 | -8.38 | 67 | -8.38 | 1 | # |
| 9 | -8.24 | 71 | -8.24 | 1 | # |
| 10 | -8.12 | 63 | -8.12 | 1 | # |
| 11 | -8.12 | 12 | -8.12 | 1 | # |
| 12 | -8.08 | 29 | -7.97 | 3 | ### |
| 13 | -8.01 | 28 | -8.01 | 1 | # |
| 14 | -7.27 | 64 | -7.27 | 1 | # |
| 15 | -7.26 | 3 | -7.26 | 1 | # |

(**A**)

FINAL GENETIC ALGORITHM DOCKED STATE

```
Detailed state:  trans 23.903 10.247 32.124 quatxyzw -0.222708 -0.830552 0.278999 -0.427486 center 3.720 -0.750 0.173 ntor 9 -174.7984 -140.1797 174.4298
70.5499 142.6159 -10.6610 -46.3666 -175.5374 8.4359
State:   23.903  10.247  32.124  -0.246 -0.919  0.309 -129.384   -174.80 -140.18  174.43   70.55  142.62  -10.66  -46.37 -175.54    8.44

DOCKED: MODEL       41
DOCKED: USER    Run = 41
DOCKED: USER    DPF = dock.dpf
DOCKED: USER
DOCKED: USER    Estimated Free Energy of Binding    =   -9.35 kcal/mol  [=(1)+(2)+(3)-(4)]
DOCKED: USER    Estimated Inhibition Constant, Ki   =  140.09 nM (nanomolar)  [Temperature = 298.15 K]
DOCKED: USER
DOCKED: USER    (1) Final Intermolecular Energy     =  -12.03 kcal/mol
DOCKED: USER        vdW + Hbond + desolv Energy     =  -11.68 kcal/mol
DOCKED: USER        Electrostatic Energy            =   -0.35 kcal/mol
DOCKED: USER    (2) Final Total Internal Energy     =   -2.58 kcal/mol
DOCKED: USER    (3) Torsional Free Energy           =   +2.68 kcal/mol
DOCKED: USER    (4) Unbound System's Energy  [=(2)] =   -2.58 kcal/mol
```

(**B**)

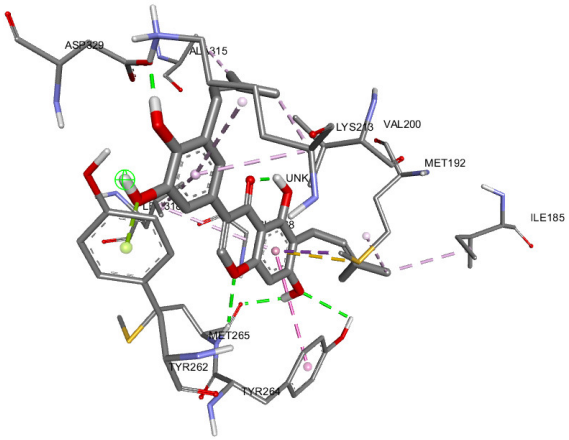


(**C**)

Preprints (www.preprints.org) | NOT PEER-REVIEWED | Posted: 24 November 2023 doi:10.20944/preprints202311.1542.v1



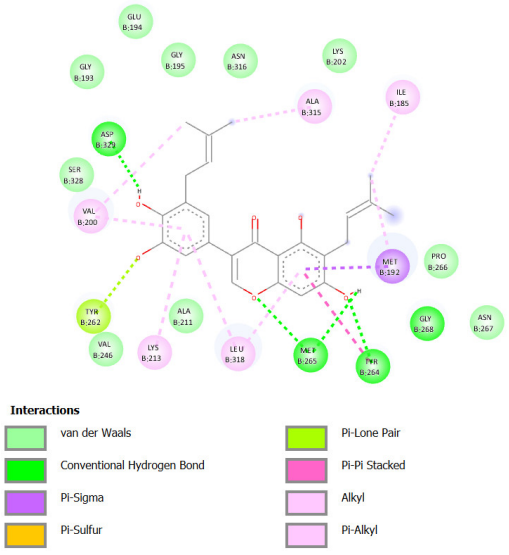


(**D**)

**Figure 8.** Docking Results of Isoangustone A with IL-1R; (**A**) Histogram of Docking Results; (**B**) Best Pose In The Molecular Docking; (**C**) 3D Shape of The Interaction As Viewed Through The *BIOVIA Discovery Studio Visualizer V.21*; (**D**) 2D Representation of The Interaction.

*Docking Results of Isoliquiritigenin with IL-1 Receptor (IL-1R)*

From the results of 100 attempts of molecular docking aimed at predicting the pose of isoliquiritigenin at the IL-1R binding site using the *Autodock Tools v.1.5.6* program, a histogram was generated, indicating that the first pose is the best pose. This is because the first pose was repeated 77 times, with the 53rd attempt being the most favorable. The binding affinity (ΔG) was calculated as -8.32 kcal/mol, and the inhibition constant was determined as 799.16 nM. Additionally, the coordinate grid point where isoliquiritigenin binds was found at x = 23.133; y = 9.735; z = 33.666.

*Docking Results of Glyzaglabrin with IL-1R*

From the results of 100 attempts of molecular docking aimed at predicting the pose of glyzaglabrin at the IL-1R binding site using the *Autodock Tools v.1.5.6* program, a histogram was obtained. This histogram indicates that the first pose is the optimal pose, as it was repeated 91 times, with the 62nd attempt being the most favorable. The calculated binding affinity (ΔG) was -8.96 kcal/mol, and the inhibition constant was found to be 270.86 nM. Additionally, the coordinate grid point where glyzaglabrin binds was found at x = 22.257; y = -9.498; z = 34.498.

*Docking Results of Prunetin with IL-1R*

From the results of 100 attempts of molecular docking aimed at predicting the pose of prunetin at the IL-1R binding site using the *Autodock Tools v.1.5.6* program, a histogram was generated. This histogram indicates that the first pose is the optimal pose, as it was repeated 99 times, with the 4th attempt being the most favorable. The calculated binding affinity (ΔG) was -8.40 kcal/mol, and the inhibition constant was found to be 691.20 nM. Additionally, the coordinate grid point where prunetin binds was found at x = 22.911; y = 9.158; z = 33.877.

*Docking Results of Shinpterocarpin with IL-1R*

From the results of 100 attempts of molecular docking aimed at predicting the pose of shinpterocarpin at the IL-1R binding site using the *Autodock Tools v.1.5.6* program, a histogram was generated. This histogram indicates that the first pose is the optimal pose, as it was repeated 67 times, with the 7th attempt being the most favorable. The calculated binding affinity (ΔG) was -9.32

 doi:10.20944/preprints202311.1542.v1



kcal/mol, and the inhibition constant was found to be 148.30 nM. Additionally, the coordinate grid point where shinpterocarpin binds was found at x = 23.008; y = 10.773; z = 33.397.

*Docking Results of Licochalcone A with IL-1R*

From the results of 100 attempts of molecular docking aimed at predicting the pose of licochalcone A at the IL-1R binding site using the *Autodock Tools v.1.5.6* program, a histogram was generated. This histogram indicates that the second pose is the optimal pose, as it was repeated 24 times, with the 38th attempt being the most favorable. The calculated binding affinity (ΔG) was -9.08 kcal/mol, and the inhibition constant was found to be 219.85 nM. Additionally, the coordinate grid point where licochalcone A binds was found at x = 23.363; y = 11.388; z = 33.273.

*Docking Results of Glabridin Withil-1R*

From the results of 100 attempts of molecular docking aimed at predicting the pose of glabridin at the IL-1R binding site using the *Autodock Tools v.1.5.6* program, a histogram was generated. This histogram indicates that the first pose is the optimal pose, as it was repeated 68 times, with the 97th attempt being the most favorable. The calculated binding affinity (ΔG) was -8.93 kcal/mol, and the inhibition constant was found to be 283.04 nM. Additionally, the coordinate grid point where glabridin binds was found at x = 24.234; y = 9.646; z = 32.454.

*Docking Results of Glisoflavone with IL-1R*

From the results of 100 attempts of molecular docking aimed at predicting the pose of Glisoflavone at the IL-1R binding site using the *Autodock Tools v.1.5.6* program, a histogram was generated. This histogram indicates that the second pose is the optimal pose, as it was repeated 36 times, with the 12th attempt being the most favorable. The calculated binding affinity (ΔG) was -9.61 kcal/mol, and the inhibition constant was found to be 90.89 nM. Additionally, the coordinate grid point where glisoflavone binds was found at x = 23.903; y = 10.431; z = 32.099.

*Docking Results of Isoangustone A with IL-1R*

From the results of 100 attempts of molecular docking aimed at predicting the pose of isoangustone A at the IL-1R binding site using the *Autodock Tools v.1.5.6 program*, a histogram was generated. This histogram indicates that the third pose is the optimal pose, as it was repeated 27 times, with the 41st attempt being the most favorable. The calculated binding affinity (ΔG) was -9.35 kcal/mol, and the inhibition constant was found to be 140.09 nM. Additionally, the coordinate grid point where isoangustone A binds was found at x = 23.903; y = 10.247; z = 32.124.

Based on the results of molecular docking through 100 trials for each ligand, it can be concluded that the eight flavonoid compounds of licorice interact with IL-1R (PDBID: 6MOM) showing highly stable bonds, indicated by the predicted values of binding affinity (ΔG) and inhibition constant (Ki). When ranking the flavonoids starting from the compound with the most stable bond to the least stable, the sequence is glisoflavone, isoangustone A, shinpterocarpin, licochalcone A, glyzaglabrin, glabridin, prunetin, and isoliquiritigenin.

*Binding Affinity and Molecular Interaction*

Table 1 provides a summary of the interaction and binding affinity between the flavonoid compounds and IL-1R.

Preprints (www.preprints.org) | NOT PEER-REVIEWED | Posted: 24 November 2023 doi:10.20944/preprints202311.1542.v1



**Table 1.** Binding affinity and molecular interaction.

| Test ligand | Binding affinity (ΔG) | Inhibition constant (Ki) | Ligand – receptor bond | | | | Run |
|---|---|---|---|---|---|---|---|
| | | | Hydrogen bond | *Van der Waals* | Hydrophobic bond (Pi) | Others | |
| Isoliquiritigenin | -8.32 kcal/mol | 799.16 nM | **Met265** **Val263** **Glu194** **Asp329** **Gly195** | **Pro266** **Gly268** **Gly193** **Tyr264** **Ser328** **Val246** **Ala315** | **Leu318** (sigma) **Ala211** (alkyl) **Tyr263** (alkyl) **Lys213** (alkyl) **Val200** (alkyl) **Met192** (alkyl) | - | 53 |
| Glyzaglabrin | -8.96 kcal/mol | 270.86 nM | **Glu233** **Lys213** | **Gly268** **Val263** **Val200** **Phe330** **Leu260** | **Asp329** (anion) **Leu318** (sigma) **Ser328** (sigma) **Tyr262** (Pi stacked) **Met192** (alkyl) **Met256** (alkyl) **Tyr264** (alkyl) **Ala211** (alkyl) **Val246** (alkyl) | - | 62 |
| Prunetin | -8.40 kcal/mol | 691.20 nM | **Val263** **Glu233** **Tyr264** | **Met265** **Gly268** **Phe330** | **Asp329** (anion) **Met192** (sigma) **Ala211** (sigma) **Leu318** (sigma) **Ser328** (sigma) **Tyr262** (Pi stacked) **Val200** (alkyl) **Val246** (alkyl) **Lys213** (alkyl) | - | 4 |
| Shinpterocarpin | -9.32 kcal/mol | 148.30 nM | **Glu233** **Asp329** **Gly268** | **Phe330** **Met265** **Gly193** **Ser269** | **Asp329** (anion) **Ser328** (sigma) **Leu318** (sigma) **Tyr262** (Pi stacked) **Val246** (alkyl) **Lys213** (alkyl) **Val200** (alkyl) **Ala211** (alkyl) **Met192** (alkyl) | - | 7 |
| Licochalcone A | -9.08 kcal/mol | 219.85 nM | **Tyr262** **Glu233** | **Glu194** **Gly193** **Ser269** **Leu319** **Phe330** | **Asp329** (anion) **Ser328** (sigma) **Leu318** (sigma) **Tyr262** (Pi stacked) **Val200** (alkyl) **Met265** (alkyl) | - | 38 |

Preprints (www.preprints.org) | NOT PEER-REVIEWED | Posted: 24 November 2023 doi:10.20944/preprints202311.1542.v1



| | | | | | | | |
|---|---|---|---|---|---|---|---|
| | | | | | **Ala211** (alkyl)<br>**Met192** (alkyl)<br>**Tyr264** (alkyl)<br>**Val246** (alkyl)<br>**Lys213** (alkyl) | | |
| Glabridin | -8.93 kcal/mol | 283.04 nM | **Asp329** | **Phe330**<br>**Met265**<br>**Ser328**<br>**Asn316**<br>**Ala315**<br>**Gly268**<br>**Pro266**<br>**Ser269** | **Met192** (sigma)<br>**Tyr262** (t-shaped)<br>**Lys213** (alkyl)<br>**Val200** (alkyl)<br>**Leu318** (alkyl)<br>**Ala211** (alkyl)<br>**Tyr264** (alkyl) | - | 97 |
| Glisoflavone | -9.61 kcal/mol | 90.89 nM | **Met265**<br>**Val263**<br>**Glu194**<br>**Asp329**<br>**Gly195** | **Pro266**<br>**Gly268**<br>**Ser328**<br>**Val246**<br>**Gly193**<br>**Ala315**<br>**Tyr264** | **Leu318** (sigma)<br>**Ala211** (alkyl) **Tyr262** (alkyl) **Lys213** (alkyl) **Val200** (alkyl) **Met192** (alkyl) | - | 41 |
| Isoangustone A | -9.35 kcal/mol | 140.09 nM | **Asp329**<br>**Met265**<br>**Tyr264**<br>**Gly268** | **Glu194**<br>**Gly193**<br>**Gly195**<br>**Asn316**<br>**Val246**<br>**Ala211**<br>**Ser328**<br>**Lys202**<br>**Pro266**<br>**Asn267** | **Met192** (sigma)<br>**Tyr262** (lone pair) **Tyr264** (Pi stacked)<br>**Val200** (alkyl)<br>**Lys213** (alkyl)<br>**Leu318** (alkyl)<br>**Ala315** (alkyl)<br>**Ile185** (alkyl)<br>**Met192** (alkyl) | - | 41 |

The results of molecular docking between the eight flavonoid compounds indicate that all tested compounds have highly stable bonds as they are lower than -7 kcal/mol. When ranked from the compound with the most stable bond to the one with the least stable, the sequence is glisoflavone, isoangustone A, shinpterocarpin, licochalcone A, glyzaglabrin, glabridin, prunetin, and isoliquiritigenin. This sequence is derived based on considerations that refer to two molecular docking parameters, namely binding affinity (ΔG) and inhibition constant (Ki). Furthermore, the analysis results of the interactions between these eight flavonoid compounds and IL-1R show that the Ki value is directly proportional to the ΔG value. Thus, the smaller the inhibition constant (Ki), the smaller was the (negative) ΔG value, and the more stable is the formed bond.

## CONCLUSIONS

From the results it can be concluded that the eight tested flavonoid compounds from the licorice plant can interact with the IL-1 receptor (IL-1R). The interactions resulting from these eight compounds exhibit strong (negative) levels of binding affinity (ΔG) and inhibition constants (Ki), indicating that the compounds form highly stable bonds with IL-1R. Furthermore, *Van der Waals* forces, hydrogen bonds, and hydrophobic bonds all contribute to the stability of these interactions. Among the eight tested compounds, glisoflavone, which has a Ki value of 90.89 nM and a ΔG value of -9.61 kcal/mol, has the highest binding affinity to IL-1R.

Further research is needed through *in vitro* and *in vivo* testing to validate the predicted interactions between the licorice flavonoids and IL-1R. This would involve investigating potential

biochemical interactions, and conducting toxicity tests on the *Glycyrrhiza glabra* flavonoids, to evaluate the safety of human consumption.

**Data Availability:** The datasets generated and/or analyzed during the current study are available in:

- Protein Data Bank Website (http://www.rscb.org) with PDBID: 6MOM
- PubChem Website (https://pubchem.ncbi.nlm.nih.gov/) with PubChem CID:
  - Isoliquiritigenin : 638278
  - Glyzaglabrin : 5317777
  - Prunetin : 5281804
  - Shinpterocarpin : 10336244
  - Licochalcone A : 5318998
  - Glabridin : 124052
  - Glisoflavone : 5487298
  - Isoangustone A : 21591148

## References


1. Petersen, P.E.; Baehni, P.C. Periodontal health and global public health. *Periodontology 2000* **2012**, *60*, 7–14.
2. World Health Organization. Oral Health: Periodontal (Gum) Disease. 2023. Available online: https://www.who.int/news-room/fact-sheets/detail/oral-health (accessed on 15 September 2023).
3. Riskesdas. Laporan Nasional Riskesdas. 2018. Available online: https://dinkes.acehprov.go.id/l-content/uploads/riskesda_2018_nasional.pdf translate (accessed on 15 September 2023).
4. Khan, S.F.; Shetty, B.; Fazal, I.; Khan, A.M.; Mir, F.M.; Moothedath, M.; et al. Licorice as A Herbal Extract in Periodontal Therapy. *Drug Target Insights* **2023**, *17*, 70–77.
5. Hajishengallis, G.; Darveau, R.P.; Curtis, M.A. The keystone-pathogen hypothesis. *Nat. Rev. Microbiol.* **2012**, *10*, 717–725.
6. Bartold, P.M.; Van Dyke, T.E. Periodontitis: A Host-Mediated Disruption of Microbial Homeostasis. Unlearning Learned Concepts. *Periodontol* **2000**, *2013*, 62, 203–217.
7. Mehrotra, N.; Singh, S. *Periodontitis* **2023**.
8. Schmidlin, P.R.; Dehghannejad, M.; Fakheran, O. Interleukin-35 Pathobiology in Periodontal Disease: A Systematic Scoping Review. *BMC Oral Health.* **2021**, *21*, 139.
9. Cheng, R.; Wu, Z.; Li, M.; Shao, M.; Hu, T. Interleukin-1β Is A Potential Therapeutic Target for Periodontitis: A Narrative Review. *Int. J. Oral Sci.* **2020**, *12*, 2.
10. Yang, R.; Yuan, B.C.; Ma, Y.S.; Zhou, S.; Liu, Y. The Anti-Inflammatory Activity of Licorice, A Widely Used Chinese Herb. *Pharm. Biol.* **2017**, *55*, 5–18.
11. Ahn, S.J.; Cho, E.J.; Kim, H.J.; Park, S.N.; Lim, Y.K.; Kook, J.K. The Antimicrobial Effects of Deglycyrrhizinated Licorice Root Extract on Streptococcus Mutans UA159 in Both Planktonic and Biofilm Cultures. *Anaerobe* **2012**, *18*, 590–596.
12. Ladke, V.S.; Kumbhar, G.M.; Joshi, K.; Kheur, S. Systemic Explanation of Glycyrrhiza Glabra's Analyzed Compounds and Anti-Cancer Mechanism Based on Network Pharmacology in Oral Cancer. *J. Oral Biosci.* **2022**, *64*, 452–460.
13. Ullah A, Munir S, Badshah SL, Khan N, Ghani L, Poulson BG; et al. Important Flavonoids and Their Role as A Therapeutic Agent. *Molecules* **2020**, *25*, 5243.
14. Leite CDos, S.; Bonafé, G.A.; Carvalho Santos, J.; Martinez, C.A.R.; Ortega, M.M.; Ribeiro, M.L. The Anti-Inflammatory Properties of Licorice (Glycyrrhiza Glabra)-Derived Compounds in Intestinal Disorders. *Int. J. Mol. Sci.* **2022**, *23*, 4121.
15. CarolineML; Muthukumar, R.S.; AHH; NN Anticancer Effect of Plectranthus Amboinicus and Glycyrrhiza Glabra on Oral Cancer Cell Line: An Invitro Experimental Study. *Asian Pac. J. Cancer Prev.* **2023**, *24*, 881–887.
16. Wahab S, Annadurai S, Abullais SS, Das G, Ahmad W, Ahmad MF; et al. Glycyrrhiza Glabra (Licorice): A Comprehensive Review on Its Phytochemistry, Biological Activities, Clinical Evidence and Toxicology. *Plants* **2021**, *10*, 2751.
17. El-Saber Batiha, G.; Magdy Beshbishy, A.; El-Mleeh, A.; M Abdel-Daim M, Prasad Devkota H. Traditional Uses, Bioactive Chemical Constituents, and Pharmacological and Toxicological Activities of Glycyrrhiza Glabra L. (Fabaceae). *Biomolecules* **2020**, *10*, 352.
18. Sharma, V.; Katiyar, A.; Agrawal, R.C. *Glycyrrhiza Glabra: Chemistry* and *Pharmacological Activity*; 2018.; pp. 87–100.

19. Tang ZH, Chen X, Wang ZY, Chai K, Wang YF, Xu XH; et al. Induction of C/EBP Homologous Protein-Mediated Apoptosis and Autophagy by Licochalcone A in Non-Small Cell Lung Cancer Cells. *Sci. Rep.* **2016**, *6*, 26241.
20. Wang J, Zhang YS, Thakur K, Hussain SS, Zhang JG, Xiao GR; et al. Licochalcone A From Licorice Root, An Inhibitor of Human Hepatoma Cell Growth Via Induction of Cell Apoptosis and Cell Cycle Arrest. *Food Chem. Toxicol.* **2018**, *120*, 407–417.
21. Bortolotto LFB, Barbosa FR, Silva G, Bitencourt TA, Beleboni RO, Baek SJ; et al. Cytotoxicity of Trans-Chalcone and Licochalcone A Against Breast Cancer Cells Is Due to Apoptosis Induction and Cell Cycle Arrest. *Biomed. Pharmacother.* **2017**, *85*, 425–433.
22. Qiu C, Zhang T, Zhang W, Zhou L, Yu B, Wang W; et al. Licochalcone A Inhibits the Proliferation of Human Lung Cancer Cell Lines A549 and H460 By Inducing G2/M Cell Cycle Arrest and ER Stress. *Int. J. Mol. Sci.* **2017**, *18*, 1761.
23. Lu WJ, Wu GJ, Chen RJ, Chang CC, Lien LM, Chiu CC; et al. Licochalcone A Attenuates Glioma Cell Growth in *Vitro* and in *Vivo* Through Cell Cycle Arrest. *Food Funct.* **2018**, *9*, 4500–4507.
24. Lin, X.; Tian, L.; Wang, L.; Li, W.; Xu, Q.; Xiao, X. Antitumor Effects and the Underlying Mechanism of Licochalcone A Combined with 5-Fluorouracil in Gastric Cancer Cells. *Oncol. Lett.* **2017**, *13*, 1695–1701.
25. Fu Y, Hsieh T Chen, Guo J, Kunicki J, Lee MYWT, Darzynkiewicz Z; et al. Licochalcone-A, A Novel Flavonoid Isolated from Licorice Root (Glycyrrhiza Glabra), Causes G2 and Late-G1 Arrests in Androgen-Independent PC-3 Prostate Cancer Cells. *Biochem. Biophys. Res. Commun.* **2004**, *322*, 263–270.
26. Chen R, Wang M, Liu Q, Wu J, Huang W, Li X; et al. Sequential Treatment with At19 Cells Generates Memory CAR-T Cells and Prolongs the Lifespan of Raji-B-NDG Mice. *Cancer Lett.* **2020**, *469*, 162–172.
27. Dabke, A.; Ghosh, S.; Dabke, P.; Sawant, K.; Khopade, A. Revisiting the In-Vitro and In-Vivo Considerations for In-Silico Modelling of Complex Injectable Drug Products. *J. Control. Release* **2023**, *360*, 185–211.
28. Nesslany, F. The Current Limitations of in Vitro Genotoxicity Testing and Their Relevance to the in Vivo Situation. *Food Chem. Toxicol.* **2017**, *106*, 609–615.
29. Ekins S, Mestres J, Testa B. *In Silico* Pharmacology for Drug Discovery: Applications to Targets and Beyond. *Br. J. Pharmacol.* **2007**, *152*, 21–37.
30. Verma, S.K.; Deshmukh, R.; Joshi, N. Molecular Biology: Fundamentals and Applications. *J. Cell Biochem.* **2020**, *122*, 230–238.
31. Guvench, O. *Small-Molecule Docking as A Structural Biology Tool*; 2020; pp. 57–86.
32. Om Silakari, Pankaj Kumar Singh. *Concepts* and *Experimental Protocols of Modelling* and *Informatics in Drug Design*; Elsevier, 2021.